Regular spectra in the vibron model with random interactions

R. Bijker[1,2] and A. Frank[2,3]

[1]*Dipartimento di Fisica, Università degli Studi di Genova, Via Dodecaneso 33, I-16146 Genova, Italy*
[2]*Instituto de Ciencias Nucleares, Universidad Nacional Autónoma de México, Apartado Postal 70-543, 04510 México, DF, México*
[3]*Centro de Ciencias Físicas, Universidad Nacional Autónoma de México, Apartado Postal 139-B, 62251 Cuernavaca, Morelos, México*

The phenomenom of emerging regular spectral features from random interactions is addressed in the context of the vibron model. A mean-field analysis links different regions of the parameter space with definite geometric shapes. The results that are, to a large extent, obtained in closed analytic form provide a clear and transparent interpretation of the high degree of order that has been observed in numerical studies.

I. INTRODUCTION

Random matrix theory was developed to describe statistical properties of nuclear spectra, such as average distributions and fluctuations of peaks in neutron-capture experiments [1,2]. In this approach, the Hamiltonian matrix elements are chosen at random, while keeping some global symmetries, e.g., the matrix should be Hermitean, and be invariant under time reversal, rotations, and reflections. Specific examples include the Gaussian orthogonal ensemble (GOE) of real-symmetric random Hamiltonian matrices in which the many-body interactions are uncorrelated, and the two-body random ensemble (TBRE) in which the two-body interactions are taken from a distribution of random numbers [3]. For two particles, the two ensembles are identical but for more than two particles, unlike the case of GOE, in TBRE the many-body matrix elements are correlated. As a consequence, also the energy eigenvalues of states with different quantum numbers are strongly correlated, since they arise from the same Hamiltonian.

The latter aspect was investigated recently in shell model calculations for even-even nuclei in the sd shell and the pf shell [4]. An analysis of the energy spectra of an ensemble of random two-body Hamiltonians showed a remarkable statistical preference for ground states with angular momentum and parity $L^P = 0^+$, despite the random nature of the two-body matrix elements, both in sign and relative magnitude. A similar preponderance of 0^+ ground states was found in an analysis of the interacting boson model (IBM) with random interactions [5]. In addition, in the IBM evidence was found for both vibrational and rotational band structures. According to the conventional ideas in the field, the occurrence of $L = 0$ ground states and the existence of vibrational and rotational bands are due to the very specific form of the interactions. Therefore these unexpected and surprising results have sparked a large number of investigations to explain and further explore the properties of random nuclei [6–19].

The basic ingredients of the numerical simulations, both for the nuclear shell model and for the IBM, are the structure of the model space, the ensemble of random Hamiltonians, the order of the interactions (one- and two-body), and the global symmetries, i.e., time-reversal, Hermiticity, and rotation and reflection symmetry. The latter three symmetries of the Hamiltonian cannot be modified, since we are studying

many-body systems whose eigenstates have real energies and good angular momentum and parity. It has been shown that the observed spectral order is a robust property that does not depend on the specific choice of the (two-body) ensemble of random interactions [4,6,7,15], the time-reversal symmetry [6], or the restriction of the Hamiltonian to one- and two-body interactions [8]. These results suggest that an explanation of the origin of the observed regular features has to be sought in the many-body dynamics of the model space and/or the general statistical properties of random interactions.

The purpose of this paper is to investigate the origin of the regular features that emerge from random interactions in a simple exactly solvable model. Hereto we use the vibron model, which is mathematically simpler than the IBM, but exhibits many of the same qualitative features. A preliminary account of this work has been published in Ref. [16]. In Sec. II we present a review of the vibron model by studying a schematic Hamiltonian with an arbitrary strength parameter. In Sec. III we discuss the spectral properties of an ensemble of random one- and two-body interactions, which are interpreted in Sec. IV in a mean-field analysis. Finally, in Sec. V we present our summary and conclusions.

II. VIBRON MODEL

The vibron model was introduced in 1981 to describe the rotational and vibrational excitations of diatomic molecules [20], and has also found applications in nuclear cluster models [21] and meson spectroscopy [22]. In general terms, it provides an algebraic treatment to describe the relative motion in two-body problems. The algebraic approach consists in quantizing the relative coordinates and momenta with vector boson operators with angular momentum and parity $L^P = 1^-$,

$$p_\mu^\dagger = \frac{1}{\sqrt{2}}\left(r_\mu - \frac{\partial}{\partial r_\mu}\right),$$

$$p_\mu = \frac{1}{\sqrt{2}}\left(r_\mu + \frac{\partial}{\partial r_\mu}\right), \tag{1}$$

and adding an auxiliary scalar boson with $L^P = 0^+$. The building blocks of the vibron model are then given by

$$s^\dagger, p^\dagger_\mu \quad (\mu = -1, 0, 1). \tag{2}$$

Sometimes, the scalar and vector bosons are also called vibrons. The 16 bilinear products of creation and annihilation operators are the generators of the Lie algebra of U(4)

$$s^\dagger s, s^\dagger p_\mu, p^\dagger_\mu s, p^\dagger_\mu p_\nu \quad (\mu, \nu = -1, 0, 1). \tag{3}$$

The Hamiltonian and all other physical operators of interest are expressed in terms of the generators. Therefore the total number of vibrons,

$$\hat{N} = s^\dagger s + \sum_\mu p^\dagger_\mu p_\mu, \tag{4}$$

is a conserved quantity. The presence of the scalar boson makes it possible to consider, in addition to the three-dimensional harmonic oscillator, also situations in which the oscillator shells are mixed. In addition to the total number of bosons N, the eigenfunctions have good angular momentum L and parity P. For a more detailed discussion of the vibron model see Ref. [23] and references therein.

A. A schematic Hamiltonian

For the study of random interactions, it is convenient to first consider a schematic Hamiltonian which contains the basic features of the model [24],

$$H = -\cos\chi\, p^\dagger \cdot \tilde{p} + \frac{\sin\chi}{4(N-1)}(s^\dagger s^\dagger - p^\dagger \cdot p^\dagger)$$

$$\times (\tilde{s}\tilde{s} - \tilde{p} \cdot \tilde{p}), \tag{5}$$

with $\tilde{s} = s$ and $\tilde{p}_\mu = (-1)^{1-\mu} p_{-\mu}$. The dots denote a scalar product with respect to the rotation group. The range of the angle χ is that of a full period $-\pi/2 < \chi \leq 3\pi/2$, such that all possible combinations of attractive and repulsive interactions are included.

For $\chi = 0, \pi$ the Hamiltonian has a U(3) dynamic symmetry. The spectrum is that of a three-dimensional harmonic oscillator, i.e., a series of oscillators shells with

$$n = 0, 1, \ldots, N,$$

$$L = n, n-2, \ldots, 1 \text{ or } 0. \tag{6}$$

The parity of the states is $P = (-1)^n = (-1)^L$. The energy spectrum is given by

$$E = \pm n, \tag{7}$$

where the $+$ $(-)$ sign corresponds to $\chi = 0$ (π).

For $\chi = \pi/2, 3\pi/2$ the Hamiltonian has an SO(4) dynamic symmetry. In this case, the harmonic oscillator shells are mixed by the Hamiltonian. The spectrum is that of a deformed or Morse oscillator, which consists of a series of rotational bands labeled by

$$\sigma = N, N-2, \ldots, 1 \text{ or } 0,$$

$$L = 0, 1, \ldots, \sigma. \tag{8}$$

The corresponding energy spectrum is given by

$$E = \pm \frac{1}{4(N-1)}(N-\sigma)(N+\sigma+2) = \pm \frac{N+1}{N-1} v\left(1 - \frac{v}{N+1}\right), \tag{9}$$

where the $+$ $(-)$ sign corresponds to $\chi = \pi/2$ $(3\pi/2)$. The ground state band has $v = (N-\sigma)/2 = 0$ for $\chi = \pi/2$ and $v = [N]/2$ for $\chi = 3\pi/2$.

B. Geometric shapes

The schematic Hamiltonian of Eq. (5) exhibits various geometric shapes (as well as the phase transitions inbetween them) which are relevant for the subsequent studies with random interactions. The connection between the vibron model, potential energy surfaces, geometric shapes, and phase transitions can be investigated by means of standard Hartree-Bose mean-field methods [24–26]. For the vibron model, it is convenient to introduce a coherent, or intrinsic, state expressed as a condensate of deformed bosons with axial symmetry,

$$|N, \alpha\rangle = \frac{1}{\sqrt{N!}}(\cos\alpha\, s^\dagger + \sin\alpha\, p^\dagger_0)^N |0\rangle, \tag{10}$$

with $0 \leq \alpha \leq \pi/2$. The potential energy surface is then given by the expectation value of the Hamiltonian in the coherent state,

$$\frac{1}{N}E(\alpha) = \frac{1}{N}\langle N, \alpha|H|N, \alpha\rangle = \cos\chi\sin^2\alpha + \frac{1}{4}\sin\chi\cos^2 2\alpha. \tag{11}$$

The equilibrium configuration is characterized by the value $\alpha = \alpha_0$ for which the potential energy surface attains its minimum value,

$$\frac{1}{N}\frac{\partial E(\alpha)}{\partial \alpha} = 0, \quad \frac{1}{N}\frac{\partial^2 E(\alpha)}{\partial \alpha^2} > 0. \tag{12}$$

The solutions can be divided into three different classes or phases:

$$\alpha_0 = 0, \quad -\pi/2 < \chi \leq \pi/4,$$

$$\cos 2\alpha_0 = \cot\chi, \quad \pi/4 \leq \chi \leq 3\pi/4,$$

$$\alpha_0 = \pi/2, \quad 3\pi/4 \leq \chi \leq 3\pi/2, \tag{13}$$

which correspond to an s-boson or spherical condensate, a deformed condensate, and a p-boson condensate, respectively (see Fig. 1). The nature of the phase transitions at the critical points $\chi_c = \pi/4, 3\pi/4$, and $3\pi/2$ can be investigated
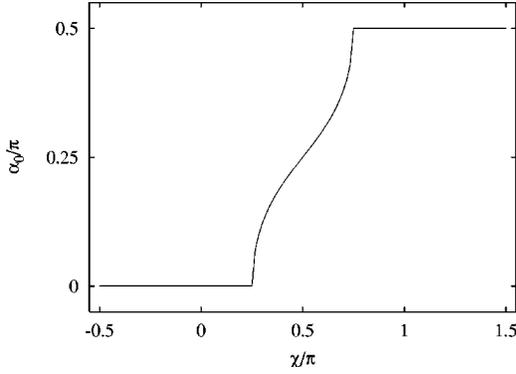
FIG. 1. Equilibrium configurations of the schematic Hamiltonian of Eq. (5) as a function of χ.

by examining the Hartree-Bose ground state energy and its derivates. The ground state energy itself is a continuous function of χ,

$$\frac{1}{N}E(\chi) = \begin{cases} \frac{1}{4}\sin\chi & -\pi/2 < \chi \leqslant \pi/4 \\ \frac{1}{2}\cos\chi - \frac{\cos^2\chi}{4\sin\chi} & \pi/4 \leqslant \chi \leqslant 3\pi/4 \\ \cos\chi + \frac{1}{4}\sin\chi & 3\pi/4 \leqslant \chi \leqslant 3\pi/2. \end{cases} \quad (14)$$

The first derivative of $E(\chi)$ shows a discontinuity at $\chi_c = 3\pi/2$, and hence the phase transition between the spherical, or s-boson, condensate and the p-boson condensate is of first order. The phase transitions involving the deformed condensate are of second order, since the second derivative of the ground state energy is discontinuous at $\chi_c = \pi/4$ and $3\pi/4$.

C. Rotations

In the previous section, we investigated the equilibrium configurations of the schematic Hamiltonian of Eq. (5). Each one of them corresponds to an intrinsic ground state band $|N, \alpha_0\rangle$, whose angular momentum content depends on the value of α_0. The rotational energies can be obtained by applying standard many-body techniques [25].

In the coherent, or intrinsic, state of Eq. (10), the rotational symmetry is spontaneously broken. In random phase approximation the corresponding spurious excitations are decoupled from the physical ones and lie at zero energy. The collective or rotational energies are then determined by the inertial parameter associated with the spurious motion,

$$E_{\text{rot}} = \frac{1}{2\mathcal{I}}L(L+1), \quad (15)$$

where the moment of inertia $\mathcal{I}$ is obtained from the Thouless-Valatin formula. The general procedure is described in Ref. [25] and applied to systems of interacting bosons in Ref. [26]. For the Hamiltonian of Eq. (5), we find that the moment of inertia is given by

$$\mathcal{I} = \frac{2N\sin^2\alpha_0}{\cos 2\alpha_0 \sin\chi}. \quad (16)$$

The ordering of the rotational energy levels is then determined by the sign of the moment of inertia. In the following, we examine each one of the equilibrium configurations in more detail.

(i) For $\alpha_0 = 0$, the equilibrium configuration has spherical symmetry, and hence can only have $L=0$. The moment of inertia is $\mathcal{I} = 0$.

(ii) For $0 < \alpha_0 < \pi/2$, the equilibrium shape is deformed. The intrinsic state is a condensate of N deformed bosons, which are superpositions of monopole and dipole bosons with $\cos 2\alpha_0 = \cot\chi$ and $\pi/4 \leqslant \chi \leqslant 3\pi/4$. The ordering of the rotational energy levels $L = 0, 1, \ldots, N$ is determined by the sign of the moment of inertia,

$$\mathcal{I} = \frac{N(\sin\chi - \cos\chi)}{\sin\chi\cos\chi}. \quad (17)$$

For $\pi/4 \leqslant \chi \leqslant \pi/2$ the moment of inertia is positive and hence the ground state has angular momentum $L=0$, whereas for for $\pi/2 \leqslant \chi \leqslant 3\pi/4$ it is negative corresponding to a ground state with $L=N$.

(iii) For $\alpha_0 = \pi/2$, the coherent state is a condensate of N dipole or p bosons. The angular momentum content is that of a three-dimensional harmonic oscillator shell with N quanta: $L = N, N-2, \ldots, 1$ or 0 for N odd or even, respectively. The moment of inertia is

$$\mathcal{I} = -\frac{2N}{\sin\chi}. \quad (18)$$

This equilibrium shape arises for $3\pi/4 \leqslant \chi \leqslant 3\pi/2$. For $3\pi/4 \leqslant \chi \leqslant \pi$, the moment of inertia is negative and the ground state has angular momentum $L=N$. For $\pi \leqslant \chi \leqslant 3\pi/2$, the moment of inertia is positive and the angular momentum of the ground state is $L=0$ for N even and $L=1$ for N odd.

In summary, the schematic Hamiltonian of Eq. (5) gives rise to three different equilibrium configurations or geometric shapes, which are separated by phase transitions. An analysis of the angular momentum content of the corresponding condensate combined with the sign of the moment of inertia yields transparent results for the ground state angular momentum. The results of Table I were obtained by assuming a constant probability distribution for χ on the interval $-\pi/2 < \chi \leqslant 3\pi/2$. The ground state is most likely to have angular momentum $L=0$: in 75% of the cases for N even and in 50% for N odd. In 25% of the cases, the ground state has the maximum value of the angular momentum $L = N$. The only other value of the ground state angular momentum is $L=1$ in 25% of the cases for N odd. The fluctuation in the $L=0$ and $L=1$ percentages is due to the contribution of the p-boson condensate. The sum of the $L=0$ and $L=1$ percentages is constant (75%) and does not depend on the total number of vibrons N.

An exact analysis in which the Hamiltonian of Eq. (5) is diagonalized numerically for different values of χ yields

TABLE I. Probabilities of ground states with $L=0$, 1, and N, obtained in a mean-field analysis of the vibron Hamiltonian of Eq. (5).

Shape		$L=0$	$L=1$	$L=N$	
$\alpha_0=0$	3/8	3/8	0	0	
$0<\alpha_0<\pi/2$	1/4	1/8	0	1/8	
$\alpha_0=\pi/2$	3/8	1/4	0	1/8	$N=2k$
	3/8	0	1/4	1/8	$N=2k+1$
Total	1	3/4	0	1/4	$N=2k$
	1	1/2	1/4	1/4	$N=2k+1$

identical results for the distribution of the ground state angular momenta as are obtained from the mean-field analysis.

III. RANDOM INTERACTIONS

In this section, we discuss the properties of the vibron model with random interactions, or more precisely, with one- and two-body interactions with random strengths. We consider the most general one- and two-body Hamiltonian of the form

$$H=\frac{1}{N}\left[H_1+\frac{1}{N-1}H_2\right],\qquad(19)$$

where H_1 contains the boson energies

$$H_1=\epsilon_s s^\dagger\cdot\tilde{s}-\epsilon_p p^\dagger\cdot\tilde{p},\qquad(20)$$

and H_2 consists of all possible two-body interactions,

$$H_2=u_0\frac{1}{2}(s^\dagger\times s^\dagger)^{(0)}\cdot(\tilde{s}\times\tilde{s})^{(0)}+u_1(s^\dagger\times p^\dagger)^{(1)}\cdot(\tilde{p}\times\tilde{s})^{(1)}$$

$$+\sum_{\lambda=0,2}c_\lambda\frac{1}{2}(p^\dagger\times p^\dagger)^{(\lambda)}\cdot(\tilde{p}\times\tilde{p})^{(\lambda)}$$

$$+v_0\frac{1}{2\sqrt{2}}[(p^\dagger\times p^\dagger)^{(0)}\cdot(\tilde{s}\times\tilde{s})^{(0)}+\text{H.c.}].\qquad(21)$$

We have scaled H_1 by N and H_2 by $N(N-1)$ in order to remove the N dependence of the matrix elements. The seven parameters of the Hamiltonian, altogether denoted by

$$(\vec{x})\equiv(\epsilon_s,\epsilon_p,u_0,u_1,c_0,c_2,v_0),\qquad(22)$$

are taken as independent random numbers on a Gaussian distribution,

$$P(x_i)=e^{-x_i^2/2\sigma^2}/\sigma\sqrt{2\pi},\qquad(23)$$

with zero mean and width σ. In this way, the interaction terms are arbitrary and equally likely to be attractive or repulsive. The spectral properties of each Hamiltonian are analyzed by exact numerical diagonalization. The results discussed in this section are based on 100 000 runs.

In Fig. 2 we show the percentages of $L=0$, $L=1$, and L
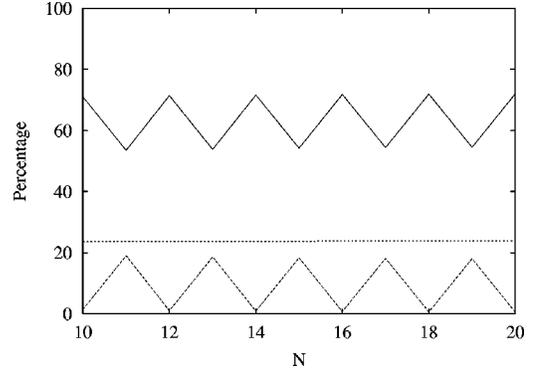
FIG. 2. Percentage of ground states with angular momentum $L=0$ (solid line), $L=1$ (dashed line), and $L=N$ (dotted line) in the vibron model with random one- and two-body interactions obtained for $10\leq N\leq 20$ and 100 000 runs.

$=N$ ground states as a function of the total number of vibrons N. The vibron model shows a dominance of $L=0$ ground states. For even values of N the ground state has $L=0$ in $\sim 71\%$ of the cases, and for odd values in $\sim 54\%$ of the cases. Similarly, the percentage of ground states with $L=1$ shows an oscillation between $\sim 1\%$ for even values of N and $\sim 18\%$ for odd values. In $\sim 24\%$ of the cases the ground state has the maximum value of the angular momentum $L=N$.

For the cases with a $L=0$ ground state, it is of interest to study the probability distribution of the ratio of excitation energies,

$$R=\frac{E_{2_1}-E_{0_1}}{E_{1_1}-E_{0_1}},\qquad(24)$$

which constitutes a measure of the spectral properties of the vibron Hamiltonian. The energy ratio R has characteristic values of $R=2$ for the vibrational or U(3) limit [harmonic oscillator, see Eq. (7)], and $R=3$ in the rotational or SO(4) limit [Morse oscillator, see Eq. (15)]. Figures 3 and 4 show that, both for odd and even values of N, the probability distribution $P(R)$ has two pronounced peaks, one at the vibrational value of $R=2$ and one at the rotational value of R
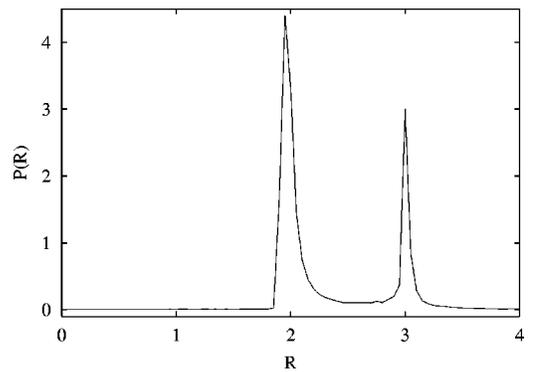
FIG. 3. Probability distribution $P(R)$ of the energy ratio R of Eq. (24) in the vibron model with random one- and two-body interactions obtained for $N=19$ and 100 000 runs.
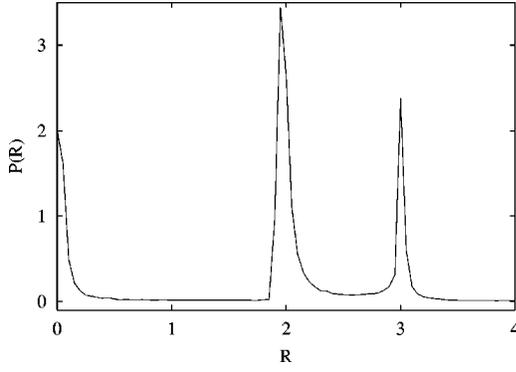
FIG. 4. As in Fig. 3, but for $N=20$.

$=3$. Moreover, for even values of N there is a maximum at $R=0$, which is absent for odd values.

These numerical results are very similar to those found for the IBM in nuclear physics [5], although there are some differences as well. Despite the random nature of the interactions both in sign and relative magnitude, the spectral properties show a surprisingly large degree of order. In recent studies, the tridiagonal form of the Hamiltonian matrix in the U(3) basis of the vibron model was used to establish a connection with random polynomials [12]. However, in general the Hamiltonian matrix is not of this form, and one has to look for alternative methods to understand the origin of these regular properties in an analytic and more intuitive way. In the next section, we apply the same mean-field techniques that were used in Sec. II, to the general one- and two-body vibron Hamiltonian of Eqs. (19)–(21) with random interaction strengths.

IV. MEAN-FIELD ANALYSIS

The potential energy surface associated with the general one- and two-body vibron Hamiltonian of Eqs. (19)–(21) is given by its expectation value in the coherent state of Eq. (10),

$$E(\alpha)=a_4\sin^4\alpha+a_2\sin^2\alpha+a_0. \qquad (25)$$

The coefficients a_i are linear combinations of the parameters of the Hamiltonian,

$$a_4=\vec{r}\cdot\vec{x}=\frac{1}{2}u_0+u_1+\frac{1}{6}c_0+\frac{1}{3}c_2+\frac{1}{\sqrt{6}}v_0,$$

$$a_2=\vec{s}\cdot\vec{x}=-\epsilon_s+\epsilon_p-u_0-u_1-\frac{1}{\sqrt{6}}v_0,$$

$$a_0=\vec{t}\cdot\vec{x}=\epsilon_s+\frac{1}{2}u_0. \qquad (26)$$

For random interaction strengths, the trial wave function of Eq. (10) and the energy surface of Eq. (25) provide information on the distribution of shapes that the model can acquire. The value of α_0 that characterizes the equilibrium configuration of the potential energy surface only depends on the
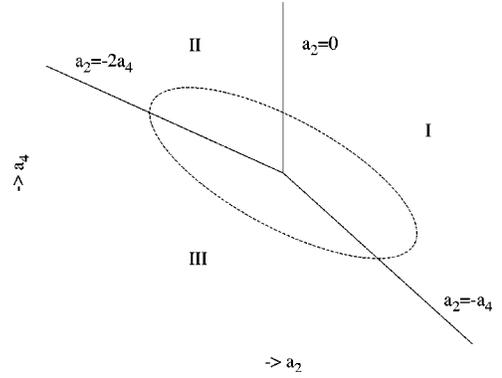
FIG. 5. Equilibrium configurations in the a_2a_4 plane: (I) spherical shape ($a_2>0,a_4>-a_2$), (II) deformed shape ($-2a_4<a_2<0$), and (III) p-boson condensate. The dashed curve corresponds to the schematic Hamiltonian of Eq. (5), and is characterized by $a_4=\sin\chi$ and $a_2=\cos\chi-\sin\chi$ with $-\pi/2<\chi\leqslant3\pi/2$.

coefficients a_4 and a_2. Just as for the schematic Hamiltonian of Eq. (5), the parameter space can be divided into different areas according to the three possible equilibrium configurations,

$$\alpha_0=0, \quad a_2>0,a_4>-a2,$$

$$\sin^2\alpha_0=-a_2/2a_4, \quad -2a_4<a_2<0,$$

$$\alpha_0=\pi/2, \quad \begin{cases} a_2<0,2a_4<-a_2 \\ a_4<-a_2<0 \end{cases}. \qquad (27)$$

In Fig. 5, the three regions in the a_2a_4 plane are labeled by I for the s-boson or spherical condensate ($\alpha_0=0$), by II for the deformed condensate ($0<\alpha_0<\pi/2$), and by III for the p-boson condensate ($\alpha_0=\pi/2$). They are separated by the separatrices $a_2=0$, $a_4>0$ for I-II, $a_2=-2a_4$, $a_4>0$ for II-III, and $a_2=-a_4$, $a_4<0$ for III-I. The dashed curve corresponds to the schematic Hamiltonian of Eq. (5), and is characterized by $a_4=\sin\chi$ and $a_2=\cos\chi-\sin\chi$ with $-\pi/2<\chi\leqslant3\pi/2$. In the previous section, we showed that this Hamiltonian exhibits three phase transitions: second order transitions at $\chi_c=\pi/4$ and $\chi_c=3\pi/4$, and a first order transition at $\chi_c=3\pi/2$. The intersections of the dashed curve and the separatrices occurs exactly at the critical points $\chi_c=\pi/4$, $3\pi/4$ and $3\pi/2$. To study the nature of the phase transitions for the case of the general Hamiltonian of Eqs. (19)–(21) we take an arbitrary ellipse in the a_2a_4 plane that encloses the origin as its center. It is straightforward to show that the order of the phase transitions does not depend on the orientation nor the eccentricity of the ellipse. In other words, the phase transitions are independent of the angle under which the separatrices are crossed.

The distribution of shapes for an ensemble of Hamiltonians depends on the joint probability distribution of the coefficients a_4 and a_2 which, for the Gaussian distribution $P(x_i)$ of Eq. (23), is given by a bivariate normal distribution,

TABLE II. Percentages of ground states with $L=0$, 1, and N, obtained in a mean-field analysis of the vibron Hamiltonian of Eqs. (19)–(21).

Shape		$L=0$	$L=1$	$L=N$	
$\alpha_0=0$	39.6%	39.6%	0.0%	0.0%	
$0<\alpha_0<\pi/2$	21.6%	13.3%	0.0%	8.3%	
$\alpha_0=\pi/2$	38.8%	17.9%	0.0%	20.9%	$N=2k$
		0.0%	17.9%	20.9%	$N=2k+1$
Total	100.0%	70.8%	0.0%	29.2%	$N=2k$
		52.9%	17.9%	29.2%	$N=2k+1$

$$P(a_4,a_2)=\int \prod_{i=1}^{7} dx_i P(x_i)\,\delta(a_4-\vec{r}\cdot\vec{x})\,\delta(a_2-\vec{s}\cdot\vec{x})$$

$$=\frac{1}{2\pi\sqrt{\det M}}\exp\left[-\frac{1}{2}\begin{pmatrix}a_4 & a_2\end{pmatrix}M^{-1}\begin{pmatrix}a_4\\a_2\end{pmatrix}\right],$$

$$(28)$$

with

$$M=\begin{pmatrix}\vec{r}\cdot\vec{r} & \vec{r}\cdot\vec{s}\\ \vec{r}\cdot\vec{s} & \vec{s}\cdot\vec{s}\end{pmatrix}=\frac{1}{18}\begin{pmatrix}28 & -30\\ -30 & 75\end{pmatrix}.\qquad (29)$$

The vectors $\vec{r}$ and $\vec{s}$ are defined in Eq. (26). The probability that the equilibrium shape of an ensemble of Hamiltonians is spherical can be obtained by integrating $P(a_4,a_2)$ over the appropriate range I ($a_2>0, a_4>-a_2$),

$$P_1=\int_I da_4 da_2 P(a_4,a_2)=\frac{1}{4\pi}\left[\pi+2\arctan\left(\frac{|\vec{s}\cdot\vec{s}+\vec{r}\cdot\vec{s}|}{\sqrt{\det M}}\right)\right]$$

$$=\frac{1}{4\pi}\left[\pi+2\arctan\sqrt{\frac{27}{16}}\right]=0.396.\qquad (30)$$

Similarly, the probability for the occurrence of a deformed shape can be derived by integrating $P(a_4,a_2)$ over the area II ($-2a_4<a_2<0$),

$$P_2=\frac{1}{2\pi}\arctan\left(\frac{2\sqrt{\det M}}{\vec{s}\cdot\vec{s}+2\vec{r}\cdot\vec{s}}\right)=\frac{1}{2\pi}\arctan\sqrt{\frac{64}{3}}=0.216.$$

$$(31)$$

Finally, the probability for finding the third solution, a p-boson condensate, is given by

$$P_3=1-P_1-P_2=0.388.\qquad (32)$$

The angular momentum of the ground state for each of the equilibrium configurations can be estimated by evaluating the moment of inertia. Just as in Sec. II, we adopt the Thouless-Valatin prescription, which leads to the formula
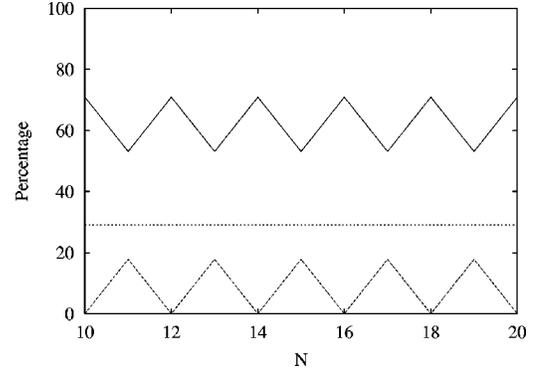
FIG. 6. Percentage of ground states with angular momentum $L=0$ (solid line), $L=1$ (dashed line), and $L=N$ (dotted line) in the vibron model with random one- and two-body interactions obtained in a mean-field analysis for $10\leq N\leq 20$.

$$\mathcal{I}=\frac{2N\sin^2\alpha_0}{4(N-1)\left[\frac{1}{2\sqrt{6}}v_0\cos^2\alpha_0-\frac{1}{6}(c_0-c_2)\sin^2\alpha_0\right]}.$$

$$(33)$$

The moment of inertia depends in a complicated way on the parameters in the Hamiltonian, both explicitly as seen in the denominator of Eq. (33) and implicitly through α_0, which determines the equilibrium configuration. For the schematic Hamiltonian of Eq. (5), it was possible to obtain a closed expression for the moment of inertia, since in this case all properties depend on a single parameter χ. However, this is not the case for the general one- and two-body Hamiltonian that we are considering here. Instead we have to solve the problem numerically.

In Table II we show the probability distribution of the ground state angular momentum as obtained in the mean-field analysis. The results are qualitatively the same as those of Table I for the schematic Hamiltonian. There is a statistical preference for $L=0$ ground states. This is largely due to the occurrence of a spherical shape (whose angular momentum content is just $L=0$) for almost 40% of the cases [see Eq. (30)]. The deformed shape yields ground states either
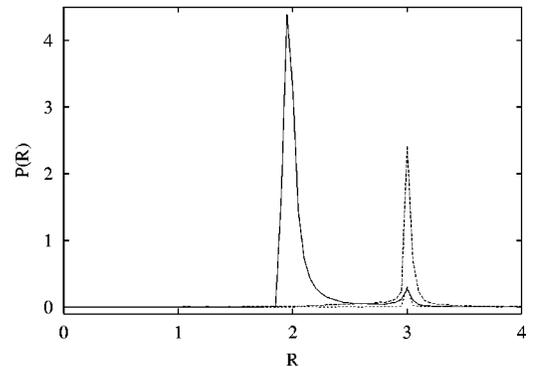
FIG. 7. Probability distribution $P(R)$ of the energy ratio R obtained for $N=19$ and 100 000 runs for the spherical (solid line), deformed (dashed line), and p-boson condensate (dotted line) equilibrium configurations, respectively.
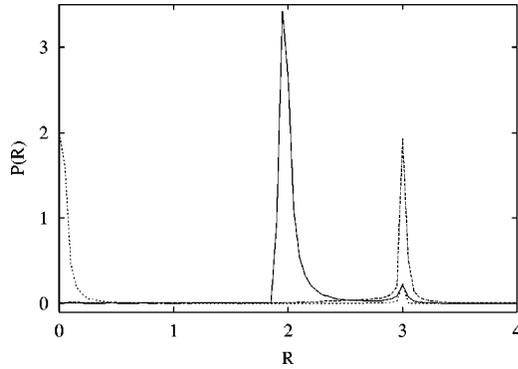
FIG. 8. As in Fig. 7, but for $N=20$.

with $L=0$ for positive values of the moment of inertia $\mathcal{I}$ >0, or with $L=N$ for $\mathcal{I}<0$. The third solution, the p-boson condensate, gives rise to ground states with $L=N$ and, depending whether the total number of vibrons is even or odd, to $L=0$ or $L=1$, respectively. The sum of the $L=0$ and $L=1$ percentages is constant. In Fig. 6 we show the percentages of $L=0$, $L=1$ and $L=N$ ground states, as a function of the total number of vibrons N. As is clear from the results presented in Table II, the fluctuations in the percentages of $L=0$ and $L=1$ ground states with N are due to the contribution from the p-boson condensate solution. A comparison with Fig. 2 shows that the mean-field results are in excellent agreement with the exact ones. The difference observed for the $L=N$ percentage arises from the fact that in the exact calculations for approximately 5% of the cases, the value of the ground state angular momentum is different from $L=0$, 1, N.

In Figs. 7 and 8 we show the contribution of each one of the equilibrium configurations to the probability distribution $P(R)$ of the energy ratio R of Eq. (24) for $N=19$ and $N=20$, respectively. For both cases, the spherical shape (solid line) contributes almost exclusively to the peak at $R=2$, and similarly the deformed shape (dashed line) to the peak at $R=3$, which confirms the vibrational and rotational character of these maxima. The occurrence of a peak at small values of R for $N=20$ corresponds to a level sequence $L=0, 2, 1$. It is related to the p-boson condensate solution (dotted line), which has angular momenta $L=N,N-2,\ldots,0$. The first excited $L=1$ state belongs to a different band and has a higher excitation energy. For odd values of N the p-boson condensate has no state with $L=0$, and hence the peak at $R=0$ is absent.

V. SUMMARY AND CONCLUSIONS

We have investigated the origin of the regular features that have been observed in numerical studies of nuclear structure models with random interactions. The observed spectral order is a robust property that arises from a much larger class of Hamiltonians than is usually thought. It cannot be explained by the time-reversal symmetry of the Hamiltonian, the choice of a specific ensemble of random interactions, or the restriction to at most two-body interactions.

In this paper, we have carried out an analysis of the vibron model, which is an exactly solvable model to describe the relative motion in two-body problems. A numerical study of the vibron model with random interactions shows the emergence of ordered features, such as the dominance of ground states with $L=0$ and the occurrence of vibrational and rotational band structures. In a mean-field analysis, it was found that different regions of the parameter space can be associated with particular intrinsic vibrational states, which in turn correspond to definite geometric shapes: a spherical shape ($\sim 40\%$), a deformed one ($\sim 20\%$), and a condensate of dipole bosons ($\sim 40\%$). Since the spherical shape only has $L=0$, and the deformed shape and the p-boson condensate with an even number of bosons N in about half the number of cases, one finds an $L=0$ ground state in approximately 70% of the cases for N even and 50% for N odd. The spherical shape gives rise to the occurrence of vibrational structure, and the deformed shape to rotational bands. Qualitatively, these results are very similar to those obtained in closed analytic form for a schematic vibron Hamiltonian which interpolates between the harmonic oscillator [or U(3) limit] and the Morse oscillator [or SO(4) limit].

In summary, the present results show that a mean-field analysis provides a clear and transparent interpretation of the regular features that have been obtained in numerical studies of the vibron model with random interactions. In Ref. [16] we have applied similar methods to the IBM. Since the structure of the model space of the IBM is more complicated than that of the vibron model, the analysis becomes more difficult, but the final results are qualitatively the same. The fact that these properties are shared by different models seems to exclude an explanation solely in terms of the angular momentum algebra, the connectivity of the model space, or the many-body dynamics of the model, as has been suggested before. The present analysis points, at least for systems of interacting bosons, to a more general phenomenon that does not depend so much on the details of the angular momentum coupling, but rather on the occurrence of definite, robust geometric phases such as spherical and deformed shapes. These shapes are a reflection of an intrinsic geometry (or topology) associated to the many-body dynamics of the model space which is sampled by the statistical nature of the random interactions, but which is quite independent of them.

For the nuclear shell model the situation is less clear. Although a large number of investigations to explain and further explore the properties of random nuclei have shed light on various aspects of the original problem, i.e., the dominance of 0^+ ground states, in our opinion, no definite answer is yet available, and the full implications for nuclear structure physics are still to be clarified.

[1] E.P. Wigner, Ann. Math. **62**, 548 (1955); **67**, 325 (1958).

[2] C.E. Porter, *Statistical Theories of Spectra: Fluctuations* (Academic, New York, 1965).

[3] T.A. Brody, J. Flores, J.B. French, P.A. Mello, A. Pandey, and S.S.M. Wong, Rev. Mod. Phys. **53**, 385 (1981); T. Guhr, A. Müller-Groeling, and H.A. Weidenmüller, Phys. Rep. **299**, 189 (1998).

[4] C.W. Johnson, G.F. Bertsch, and D.J. Dean, Phys. Rev. Lett. **80**, 2749 (1998).

[5] R. Bijker and A. Frank, Phys. Rev. Lett. **84**, 420 (2000).

[6] R. Bijker, A. Frank, and S. Pittel, Phys. Rev. C **60**, 021302(R) (1999).

[7] C.W. Johnson, G.F. Bertsch, D.J. Dean, and I. Talmi, Phys. Rev. C **61**, 014311 (2000).

[8] R. Bijker and A. Frank, Phys. Rev. C **62**, 014303 (2000).

[9] R. Bijker, A. Frank, and S. Pittel, Rev. Mex. Fis. **46 S1**, 47 (2000).

[10] D. Kusnezov, N.V. Zamfir, and R.F. Casten, Phys. Rev. Lett. **85**, 1396 (2000).

[11] D. Mulhall, A. Volya, and V. Zelevinsky, Phys. Rev. Lett. **85**, 4016 (2000).

[12] D. Kusnezov, Phys. Rev. Lett. **85**, 3773 (2000); R. Bijker and A. Frank, *ibid.* **87**, 029201 (2001); D. Kusnezov, *ibid.* **87**, 029202 (2001).

[13] S. Drożdż and M. Wójcik, Physica A **301**, 291 (2001).

[14] Y.M. Zhao and A. Arima, Phys. Rev. C **64**, 041301(R) (2001).

[15] D. Dean, Nucl. Phys. **A682**, 194c (2001).

[16] R. Bijker and A. Frank, Phys. Rev. C **64**, 061303(R) (2001).

[17] R. Bijker and A. Frank, Nucl. Phys. News **11** (4), 15 (2001).

[18] P. Chau Huu-Tai, N.A. Smirnova, and P. van Isacker, preprint GANIL P-01-11.

[19] V. Velázquez and A.P. Zuker, Phys. Rev. Lett. **88**, 072502 (2002).

[20] F. Iachello, Chem. Phys. Lett. **78**, 581 (1981); F. Iachello and R.D. Levine, J. Chem. Phys. **77**, 3046 (1982).

[21] F. Iachello, Phys. Rev. C **23**, 2778 (1981).

[22] F. Iachello, N.C. Mukhopadhyay, and L. Zhang, Phys. Rev. D **44**, 898 (1991).

[23] F. Iachello and R.D. Levine, *Algebraic Theory of Molecules* (Oxford University Press, Oxford, 1995).

[24] O.S. van Roosmalen and A.E.L. Dieperink, Ann. Phys. (N.Y.) **139**, 198 (1982); O. S. van Roosmalen, Ph.D. thesis, Universitat Groningen, 1982.

[25] P. Ring and P. Schuck, *The Nuclear Many-Body Problem* (Springer Verlag, New York, 1980).

[26] J. Dukelsky, G.G. Dussel, R.P.J. Perazzo, S.L. Reich, and H.M. Sofia, Nucl. Phys. **A425**, 93 (1984).